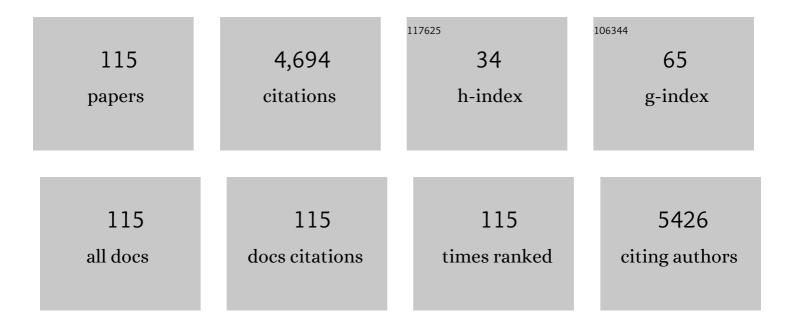
List of Publications by Year in descending order

Source: https://exaly.com/author-pdf/1965961/publications.pdf Version: 2024-02-01



#	Article	IF	CITATIONS
1	White light emission from a single organic molecule with dual phosphorescence at room temperature. Nature Communications, 2017, 8, 416.	12.8	621
2	Construction of Efficient Deep Blue Aggregation-Induced Emission Luminogen from Triphenylethene for Nondoped Organic Light-Emitting Diodes. Chemistry of Materials, 2015, 27, 3892-3901.	6.7	208
3	Enhancing Thermal Stability and Living Fashion in α-Diimine–Nickel-Catalyzed (Co)polymerization of Ethylene and Polar Monomer by Increasing the Steric Bulk of Ligand Backbone. Macromolecules, 2017, 50, 2675-2682.	4.8	195
4	Longâ€Lived Roomâ€Temperature Phosphorescence for Visual and Quantitative Detection of Oxygen. Angewandte Chemie - International Edition, 2019, 58, 12102-12106.	13.8	195
5	Electrical behavior of polypropylene/multiwalled carbon nanotube nanocomposites with low percolation threshold. Scripta Materialia, 2007, 57, 461-464.	5.2	158
6	Synthesis and Characterization of Organometallic Coordination Polymer Nanoshells of Prussian Blue Using Miniemulsion Periphery Polymerization (MEPP). Journal of the American Chemical Society, 2009, 131, 5378-5379.	13.7	150
7	Polyethylene/maleic anhydride grafted polyethylene/organic-montmorillonite nanocomposites. I. Preparation, microstructure, and mechanical properties. Journal of Applied Polymer Science, 2004, 91, 3974-3980.	2.6	138
8	A mechanistic study of AIE processes of TPE luminogens: intramolecular rotation vs. configurational isomerization. Journal of Materials Chemistry C, 2016, 4, 99-107.	5.5	132
9	Molecular luminogens based on restriction of intramolecular motions through host–guest inclusion for cell imaging. Chemical Communications, 2014, 50, 1725-1727.	4.1	129
10	Effect of mechanical stretching on electrical conductivity and positive temperature coefficient characteristics of poly(vinylidene fluoride)/carbon nanofiber composites prepared by non-solvent precipitation. Carbon, 2011, 49, 1758-1768.	10.3	116
11	Preparation and crystallization behaviour of PP/PP-g-MAH/Org-MMT nanocomposite. European Polymer Journal, 2003, 39, 1467-1474.	5.4	107
12	Electrical properties of low-density polyethylene/multiwalled carbon nanotube nanocomposites. Materials Chemistry and Physics, 2006, 100, 132-137.	4.0	106
13	Facile Synthesis of Efficient Luminogens with AIE Features for Threeâ€Photon Fluorescence Imaging of the Brain through the Intact Skull. Advanced Materials, 2020, 32, e2000364.	21.0	103
14	Stepwise Energy Transfer: Nearâ€Infrared Persistent Luminescence from Doped Polymeric Systems. Advanced Materials, 2022, 34, e2108333.	21.0	97
15	Electrical properties of low-density polyethylene/ZnO nanocomposites. Materials Chemistry and Physics, 2006, 100, 1-5.	4.0	86
16	Microstructure and properties of polypropylene composites filled with silver and carbon nanotube nanoparticles prepared by melt-compounding. Materials Science and Engineering B: Solid-State Materials for Advanced Technology, 2007, 142, 55-61.	3.5	83
17	Polypropylene/montmorillonite nanocomposites toughened with SEBS-g-MA: Structure-property relationship. Journal of Polymer Science, Part B: Polymer Physics, 2005, 43, 3112-3126.	2.1	82
18	PP-PP-g-MAH-Org-MMT nanocomposites. I. Intercalation behavior and microstructure. Journal of Applied Polymer Science, 2003, 88, 3225-3231.	2.6	78

#	Article	IF	CITATIONS
19	Red emissive AIE luminogens with high hole-transporting properties for efficient non-doped OLEDs. Chemical Communications, 2015, 51, 7321-7324.	4.1	76
20	Ligand-Directed Regioselectivity in Amine–Imine Nickel-Catalyzed 1-Hexene Polymerization. ACS Catalysis, 2015, 5, 122-128.	11.2	70
21	Sensitive and reliable detection of glass transition of polymers by fluorescent probes based on AIE luminogens. Polymer Chemistry, 2015, 6, 3537-3542.	3.9	64
22	Crystallization-Induced Hybrid Nano-Sheets of Fluorescent Polymers with Aggregation-Induced Emission Characteristics for Sensitive Explosive Detection. ACS Macro Letters, 2014, 3, 21-25.	4.8	63
23	PE/PE-g-MAH/Org-MMT nanocomposites. II. Nonisothermal crystallization kinetics. Journal of Applied Polymer Science, 2004, 91, 3054-3059.	2.6	53
24	Temperature-induced and crystallization-driven self-assembly of polyethylene-b-poly(ethylene oxide) in solution. Polymer, 2013, 54, 1663-1670.	3.8	53
25	Bioinspired Fluorescent Nanosheets for Rapid and Sensitive Detection of Organic Pollutants in Water. ACS Sensors, 2016, 1, 1272-1278.	7.8	52
26	Positive Temperature Coefficient Effect of Polypropylene/Carbon Nanotube/Montmorillonite Hybrid Nanocomposites. IEEE Nanotechnology Magazine, 2009, 8, 729-736.	2.0	51
27	Poly(propylene)-poly(propylene)-grafted maleic anhydride-organic montmorillonite (PP-PP-g-MAH-Org-MMT) nanocomposites. II. Nonisothermal crystallization kinetics. Journal of Applied Polymer Science, 2003, 88, 3093-3099.	2.6	45
28	Longâ€Lived Roomâ€Temperature Phosphorescence for Visual and Quantitative Detection of Oxygen. Angewandte Chemie, 2019, 131, 12230-12234.	2.0	44
29	Crystallization and coalescence of block copolymer micelles in semicrystalline block copolymer/amorphous homopolymer blends. Polymer, 2005, 46, 1709-1716.	3.8	42
30	Glass transition of polystyrene nanospheres under different confined environments in aqueous dispersions. Soft Matter, 2013, 9, 4614.	2.7	42
31	Effects of crystallization on dispersion of carbon nanofibers and electrical properties of polymer nanocomposites. Polymer Engineering and Science, 2008, 48, 177-183.	3.1	41
32	Electrical properties of percolative polystyrene/carbon nanofiber composites. IEEE Transactions on Dielectrics and Electrical Insulation, 2008, 15, 214-220.	2.9	40
33	Research on 5-fluorouracil as a drug carrier materials with its in vitro release properties on organic modified magadiite. European Journal of Pharmaceutical Sciences, 2019, 130, 44-53.	4.0	40
34	Effects of Cationic Species in Salts on the Electrical Conductivity of Doped PEDOT:PSS Films. ACS Applied Polymer Materials, 2021, 3, 98-103.	4.4	40
35	General Platform for Remarkably Thermoresponsive Fluorescent Polymers with Memory Function. ACS Macro Letters, 2016, 5, 909-914.	4.8	35
36	Synthesis and self-assembly of isotactic polystyrene-block-poly(ethylene glycol). Polymer Chemistry, 2013, 4, 954-960.	3.9	33

#	Article	IF	CITATIONS
37	A novel stimuli-responsive fluorescent elastomer based on an AIE mechanism. Polymer Chemistry, 2015, 6, 8194-8202.	3.9	33
38	Sensitive and rapid detection of aliphatic amines in water using self-stabilized micelles of fluorescent block copolymers. Journal of Hazardous Materials, 2019, 368, 630-637.	12.4	33
39	Simultaneous promotion of efficiency and lifetime of organic phosphorescence for self-referenced temperature sensing. Chemical Engineering Journal, 2020, 400, 125934.	12.7	32
40	Electrical properties of low density polyethylene/ZnO nanocomposites: The effect of thermal treatments. Journal of Applied Polymer Science, 2006, 102, 1436-1444.	2.6	31
41	Adsorption Analyses of Phenol from Aqueous Solutions Using Magadiite Modified with Organo-Functional Groups: Kinetic and Equilibrium Studies. Materials, 2019, 12, 96.	2.9	31
42	Alternating Vinylarene–Carbon Monoxide Copolymers: Simple and Efficient Nonconjugated Luminescent Macromolecules. Macromolecules, 2020, 53, 9337-9344.	4.8	30
43	Preparation and Characterization of Magadiite–Magnetite Nanocomposite with Its Sorption Performance Analyses on Removal of Methylene Blue from Aqueous Solutions. Polymers, 2019, 11, 607.	4.5	29
44	Thin Film Morphology of Symmetric Semicrystalline Oxyethylene/Oxybutylene Diblock Copolymers on Silicon. Macromolecules, 2006, 39, 5471-5478.	4.8	26
45	Catalytic synthesis of polyethylene-block-polynorbornene copolymers using a living polymerization nickel catalyst. Polymer Chemistry, 2014, 5, 6012-6018.	3.9	26
46	Rapid detection of aromatic pollutants in water using swellable micelles of fluorescent polymers. Sensors and Actuators B: Chemical, 2019, 283, 415-425.	7.8	25
47	A mass-amplifying electrochemiluminescence film (MAEF) for the visual detection of dopamine in aqueous media. Nanoscale, 2020, 12, 8828-8835.	5.6	25
48	Synthesis of amphiphilic polyethylene-b-poly(l-glutamate) block copolymers with vastly different solubilities and their stimuli-responsive polymeric micelles in aqueous solution. Polymer, 2014, 55, 4593-4600.	3.8	23
49	Synthesis of well-defined amphiphilic branched polyethylene-graft-poly (N-isopropylacrylamide) copolymers by coordination copolymerization in tandem with RAFT polymerization and their self-assembled vesicles. Polymer Chemistry, 2014, 5, 962-970.	3.9	23
50	Sticky nanopads made of crystallizable fluorescent polymers for rapid and sensitive detection of organic pollutants in water. Journal of Materials Chemistry A, 2017, 5, 2115-2122.	10.3	23
51	Quantitative and rapid detection of explosives using an efficient luminogen with aggregation-induced emission characteristics. Sensors and Actuators B: Chemical, 2020, 302, 127201.	7.8	23
52	Preparation of organic-modified magadiite–magnetic nanocomposite particles as an effective nanohybrid drug carrier material for cancer treatment and its properties of sustained release mechanism by Korsmeyer–Peppas kinetic model. Journal of Materials Science, 2021, 56, 14270-14286.	3.7	22
53	Full-type photoluminescence from a single organic molecule for multi-signal temperature sensing. Materials Chemistry Frontiers, 2021, 5, 2261-2270.	5.9	22
54	Synthesis, characterization and micellization of amphiphilic polyethylene-b-polyphosphoester block copolymers. RSC Advances, 2015, 5, 49376-49384.	3.6	21

#	Article	IF	CITATIONS
55	Continuously-tunable fluorescent polypeptides through a polymer-assisted assembly strategy. Polymer Chemistry, 2016, 7, 5181-5187.	3.9	21
56	Curing behavior of epoxy resin/tung oil anhydride exfoliated nanocomposite by differential scanning calorimetry. Journal of Applied Polymer Science, 2004, 92, 3822-3829.	2.6	20
57	Electrical Conducting Behavior of Polyethylene Composites Filled with Selfâ€Passivated Aluminum Nanoparticles and Carbon Nanotubes. Advanced Engineering Materials, 2007, 9, 1014-1017.	3.5	18
58	Bright electrochemiluminescent films of efficient aggregation-induced emission luminogens for sensitive detection of dopamine. Materials Chemistry Frontiers, 2019, 3, 2051-2057.	5.9	18
59	Synthesis and characterization of ultrathin metal coordination Prussian blue nanoribbons. Dalton Transactions, 2013, 42, 5242.	3.3	17
60	Glass transition of poly(methyl methacrylate) nanospheres in aqueous dispersion. Physical Chemistry Chemical Physics, 2014, 16, 15941.	2.8	17
61	Thermoresponsive Fluorescent Semicrystalline Polymers Decorated with Aggregation Induced Emission Luminogens. Chinese Journal of Polymer Science (English Edition), 2019, 37, 394-400.	3.8	17
62	Preparation of waterborne polyurethane with high solid content and elasticity. Journal of Polymer Research, 2019, 26, 1.	2.4	16
63	Self-Amplified Fluorescent Nanoparticles for Rapid and Visual Detection of Xylene in Aqueous Media. ACS Sensors, 2019, 4, 2536-2545.	7.8	15
64	Effect of Substrate Surface on Dewetting Behavior and Chain Orientation of Semicrystalline Block Copolymer Thin Films. Journal of Physical Chemistry B, 2006, 110, 24384-24389.	2.6	14
65	Lamellar Orientation in Thin Films of Symmetric Semicrytalline Polystyrene- <i>b</i> -poly(ethylene- <i>co</i> -butene) Block Copolymers:  Effects of Molar Mass, Temperature of Solvent Evaporation, and Annealing. Journal of Physical Chemistry B, 2007, 111, 11921-11928.	2.6	14
66	Crystalline-coil diblock copolymers of syndiotactic polypropylene-b- poly(ethylene oxide): synthesis, solution self-assembly, and confined crystallization in nanosized micelle cores. Journal of Polymer Research, 2013, 20, 1.	2.4	14
67	Crystallization-Induced Redox-Active Nanoribbons of Organometallic Polymers. ACS Macro Letters, 2015, 4, 593-597.	4.8	14
68	Bathochromic-Shifted Emissions by Postfunctionalization of Nonconjugated Polyketones. ACS Applied Materials & Interfaces, 2021, 13, 59288-59297.	8.0	14
69	Strainâ€Responsive Persistent Roomâ€Temperature Phosphorescence from Halogenâ€Free Polymers for Early Damage Reporting through Phosphorescence Lifetime and Image Analysis. Advanced Optical Materials, 2022, 10, .	7.3	14
70	Effect of Substrate and Molecular Weight on the Stability of Thin Films of Semicrystalline Block Copolymers. Langmuir, 2007, 23, 3673-3679.	3.5	13
71	Morphology of semicrystalline oxyethylene/oxybutylene block copolymer thin films on mica. Polymer, 2007, 48, 7201-7210.	3.8	13
72	Amphiphilic Nanocapsules Entangled with Organometallic Coordination Polymers for Controlled Cargo Release. Langmuir, 2014, 30, 6294-6301.	3.5	13

5

#	Article	IF	CITATIONS
73	Deepâ€Blue Ultralong Roomâ€Temperature Phosphorescence from Halogenâ€Free Organic Materials through Cage Effect for Various Applications. Advanced Optical Materials, 2021, 9, 2100959.	7.3	13
74	Polarized optical microscopy study on the superstructures of oxyethylene/oxybutylene block copolymers. Polymer, 2004, 45, 6675-6680.	3.8	12
75	The Synthesis of Organometallic Coordination Polymer Flowers of Prussian Blue with Ultrathin Petals by Using Crystallizationâ€Assisted Interface Coordination Polymerization (CAICP). Chemistry - A European Journal, 2012, 18, 15272-15276.	3.3	12
76	Confined crystallization of core-forming blocks in nanoscale self-assembled micelles of poly(Îμ-caprolactone)-b-poly(ethylene oxide) in aqueous solution. Journal of Polymer Research, 2013, 20, 1.	2.4	11
77	Graphene-induced tiny flowers of organometallic polymers with ultrathin petals for hydrogen peroxide sensing. Carbon, 2015, 93, 719-730.	10.3	11
78	Systemic research of fluorescent emulsion systems and their polymerization process with a fluorescent probe by an AIE mechanism. RSC Advances, 2016, 6, 74225-74233.	3.6	11
79	Glass transition and quantum yield for fluorescent labelled polystyrene core-forming block in self-assembled nanomicelles of amphiphilic diblock copolymers. Journal of Polymer Research, 2015, 22, 1.	2.4	10
80	Synthesis and Characterization of Nanowire Coils of Organometallic Coordination Polymers for Controlled Cargo Release. Journal of Physical Chemistry B, 2014, 118, 6339-6345.	2.6	9
81	Growing Tiny Flowers of Organometallic Polymers along Carbon Nanotubes. Macromolecules, 2015, 48, 4115-4121.	4.8	9
82	Adsorption Process and Properties Analyses of a Pure Magadiite and a Modified Magadiite on Rhodamine-B from an Aqueous Solution. Processes, 2019, 7, 565.	2.8	9
83	Nonisothermal crystallization kinetics of lowâ€density polyethylene inside percolating network of ZnO nanoparticles. Journal of Applied Polymer Science, 2012, 125, E113.	2.6	8
84	Effects on the Mechanical Properties of Nacre-Like Bio-Hybrid Membranes with Inter-Penetrating Petal Structure Based on Magadiite. Materials, 2019, 12, 173.	2.9	8
85	Crystallization and melting behaviors of polystyrene-b-poly(ethylene-co-butene) block copolymers. European Polymer Journal, 2007, 43, 3153-3162.	5.4	7
86	Poly(γ-benzyl-l-glutamate) decorated with cyanoferrate complex: synthesis, characterization and electrochemical properties. Polymer Chemistry, 2013, 4, 3821.	3.9	7
87	Waterborne redox-active helix–coil–helix triblock metallopolymers: Synthesis, disassembly and electrochemical behaviors. Polymer, 2014, 55, 2205-2212.	3.8	7
88	Crystallization-driven self-assembly of isotactic polystyrene in N, N-dimethylformamide. Chinese Journal of Polymer Science (English Edition), 2015, 33, 646-651.	3.8	7
89	Synthesis and self-assembly in aqueous solution of amphiphilic diblock copolymers containing hyperbranched polyethylene. Polymer, 2015, 57, 125-131.	3.8	7
90	Study on glass transition and physical aging of polystyrene nanowires by differential scanning calorimetry. Journal of Polymer Research, 2017, 24, 1.	2.4	7

#	Article	IF	CITATIONS
91	The influences of electronic effect and isomerization of salalen titanium( <scp>iv</scp> ) complexes on ethylene polymerization in the presence of methylaluminoxane. RSC Advances, 2019, 9, 41824-41831.	3.6	7
92	Conjugated microporous polymers for near-infrared photothermal control of shape change. Science China Materials, 2021, 64, 430-439.	6.3	7
93	Synthesis of polystyrene-b-poly(ethylene-co-butene) block copolymers by anionic living polymerization and subsequent noncatalytic hydrogenation. Journal of Applied Polymer Science, 2006, 102, 2632-2638.	2.6	6
94	Metal coordination induced disassembly of polypeptides affords electrochemically active hybrid nano-helices. Polymer Chemistry, 2013, 4, 5671.	3.9	6
95	Study on the condensed state physics of poly( $\hat{l}\mu$ -caprolactone) nano-aggregates in aqueous dispersions. Journal of Colloid and Interface Science, 2015, 450, 264-271.	9.4	6
96	Investigation on the Preparation and Properties of CMC/magadiite Nacre-Like Nanocomposite Films. Polymers, 2019, 11, 1378.	4.5	6
97	Transformable fluorescent nanoparticles (TFNs) of amphiphilic block copolymers for visual detection of aromatic amines in water. Polymer Chemistry, 2021, 12, 5467-5476.	3.9	6
98	Preparation of Magadiite-Sodium Alginate Drug Carrier Composite by Pickering-Emulsion-Templated-Encapsulation Method and Its Properties of Sustained Release Mechanism by Baker–Lonsdale and Korsmeyer–Peppas Model. Journal of Polymers and the Environment, 2022, 30, 3890-3900.	5.0	6
99	Crystallization of lowâ€density polyethylene embedded inside zinc oxide nanoparticle percolating network. Polymer Engineering and Science, 2012, 52, 1250-1257.	3.1	5
100	Fluorescent quantum yield of pyrene probe in ultrathin polymer films. Chinese Journal of Polymer Science (English Edition), 2017, 35, 400-406.	3.8	5
101	Dual-potential electrochemiluminescent film constructed from single AIE luminogens for the sensitive detection of malachite green. Nanoscale, 2022, 14, 7711-7719.	5.6	5
102	Comparison of Crystallization Rate and Macroscopic Morphology of Two Oxyethylene/Oxybutylene Triblock Copolymers. The Effect of Molecular Architecture. Polymer Journal, 2004, 36, 465-471.	2.7	4
103	Large-scale synthesis of organometallic polymer flowers with ultrathin petals for hydrogen peroxide sensing. Polymer Chemistry, 2015, 6, 4447-4454.	3.9	4
104	Tiny nanoparticles of organometallic polymers through the direct disassembly-assisted synthesis strategy for hydrogen peroxide sensing. Polymer Chemistry, 2015, 6, 7179-7187.	3.9	4
105	Synthesis and self-assembly of a novel amphiphilic diblock copolymer consisting of isotactic polystyrene and 1,4-trans-polybutadiene-graft-poly(ethylene oxide). RSC Advances, 2018, 8, 12752-12759.	3.6	4
106	Fluorescent nanoparticles of amphiphilic block copolymers for sensitive and rapid detection of N-ethylaniline in water. Dyes and Pigments, 2021, 190, 109333.	3.7	4
107	Melting–Recrystallization of Block Copolymer Crystals in Confined Environments. Polymer Journal, 2005, 37, 43-46.	2.7	3
108	Syndiospecific polymerization of styrene with C1-symmetric [OSNO]-typeÂbridged bis(phenolate) titanium (IV) complexes. Journal of Organometallic Chemistry, 2015, 798, 347-353.	1.8	3

#	Article	IF	CITATIONS
109	Synthesis of isotactic polystyrene-block-polyethylene by the combination of sequential monomer addition and hydrogenation of 1,4-trans-polybutadiene block. Chinese Journal of Polymer Science (English Edition), 2017, 35, 866-873.	3.8	3
110	Theoretical Aspects of Polymer Crystallization in Multiphase Systems. , 2018, , 17-48.		2
111	Title is missing!. Chinese Journal of Polymer Science (English Edition), 2006, 24, 341.	3.8	2
112	Fabrication and electrical conducting behavior of carbon nanofiber reinforced high-density polyethylene/ polystyrene nanocomposites with low percolation threshold. E-Polymers, 2008, 8, .	3.0	1
113	Synthesis and characterization of isotactic poly(p-hydroxystyrene)- block-1,4-trans-polybutadiene by sequential monomer addition using titanium complex with an [OSSO]-type Bis(phenolate) ligand. Journal of Polymer Research, 2019, 26, 1.	2.4	1
114	A flexible and bright surface-enhanced electrochemiluminescence film constructed from efficient aggregation-induced emission luminogens for biomolecular sensing. Journal of Materials Chemistry B, 2022, , .	5.8	1
115	Electrical Behavior of High Density Polyethylene/ZnO Nano-composites. E-Polymers, 2007, 7, .	3.0	0